PHYSICAL REVIEW B **92**, 020505(R) (2015)

Enhancement of low-frequency fluctuations and superconductivity breakdown in Mn-doped $La_{1-y}Y_yFeAsO_{0.89}F_{0.11}$ superconductors

F. Hammerath,[1,2,3] M. Moroni,[1] L. Bossoni,[1,4] S. Sanna,[1] R. Kappenberger,[2] S. Wurmehl,[2,3] A. U. B. Wolter,[2,3] M. A. Afrassa,[2,5] Y. Kobayashi,[6] M. Sato,[7] B. Büchner,[2,3] and P. Carretta[1]

[1]*Department of Physics, University of Pavia-CNISM, I-27100 Pavia, Italy*
[2]*Leibniz-Institut für Festkörper- und Werkstoffforschung (IFW) Dresden, 01171 Dresden, Germany*
[3]*Institute for Solid State Physics, Dresden Technical University, TU-Dresden, 01062 Dresden, Germany*
[4]*Kamerlingh Onnes Laboratory, University of Leiden, 2300 RA Leiden, The Netherlands*
[5]*Addis Ababa University, College of Natural Science, Addis Ababa, Ethiopia*
[6]*Department of Physics, Division of Material Science, Nagoya University, Nagoya 464-8602, Japan*
[7]*Research Center for Neutron Science and Technology, CROSS, 162-1 Shirakata, Tokai 319-1106 Japan*

(Received 12 April 2015; revised manuscript received 10 June 2015; published 13 July 2015)

^{19}F NMR measurements in optimally electron-doped $La_{1-y}Y_yFe_{1-x}Mn_xAsO_{0.89}F_{0.11}$ superconductors are presented. The effect of Mn doping on the superconducting phase is studied for two series of compounds ($y = 0$ and $y = 0.2$) where the chemical pressure is varied by substituting La with Y. In the $y = 0.2$ series superconductivity is suppressed for Mn contents an order of magnitude larger than for $y = 0$. For both series a peak in the ^{19}F NMR nuclear spin-lattice relaxation rate $1/T_1$ emerges upon Mn doping and becomes significantly enhanced on approaching the quantum phase transition between the superconducting and magnetic phases. ^{19}F NMR linewidth measurements show that for similar Mn contents magnetic correlations are more pronounced in the $y = 0$ series, at variance with what one would expect for $\vec{Q} = (\pi/a,0)$ spin correlations. These observations suggest that Mn doping tends to reduce fluctuations at $\vec{Q} = (\pi/a,0)$ and to enhance other low-frequency modes. The effect of this transfer of spectral weight on the superconducting pairing is discussed along with the charge localization induced by Mn.

DOI: 10.1103/PhysRevB.92.020505 PACS number(s): 74.70.Xa, 76.60.−k, 76.75.+i, 74.40.Kb

The introduction of impurities in superconducting materials is a well known approach to test their stability for future technological applications as well as to unravel their intrinsic microscopic properties. In the cuprates the study of the staggered spin configuration around isolated spinless impurities, as Zn, has allowed one to determine how the electronic correlations evolve throughout the phase diagram [1]. When a sizable amount of impurities is introduced they can no longer be treated as independent local perturbations; the correlation among the impurities themselves has to be considered and quantum transitions to new phases may arise [2].

In iron-based superconductors several studies on the effect of impurities have been carried out and it has soon emerged that the behavior may vary a lot depending on the family considered. If one concentrates on the $LnFeAsO_{1-z}F_z$ (Ln1111) family, with Ln a lanthanide ion, one notices that spinless impurities introduced by substituting Fe by Ru, cause a very weak effect both on the magnetic ($z = 0$) [3–6] and on the superconducting ($z = 0.11$) [7–11] ground state. One has to introduce almost 60% of Ru to quench either one of the two phases. On the other hand, if one considers the effect of paramagnetic impurities such as Mn [12] a much stronger effect is observed. In fact, in optimally doped ($z \simeq 0.11$) Sm1111 the superconducting transition temperature T_c vanishes for a Mn content around 8% (see Fig. 1). Remarkably in optimally electron-doped $LaFe_{1-x}Mn_xAsO_{0.89}F_{0.11}$ superconductors T_c drops to zero for x as low as 0.2% [13], more than an order of magnitude less than for Sm1111, and a quantum phase transition to a magnetic ground state is observed [14]. The different behavior of Sm1111 and La1111 against Mn impurities shows that by decreasing the lanthanide ion size T_c decreases more slowly with x and the system is driven away from a quantum critical point (QCP).

The nature of the magnetic ground state developing at high Mn contents is still controversial [15]. In $Ba_{0.5}K_{0.5}(Fe_{1-x}Mn_xAs)_2$ superconductors neutron scattering results suggested that Mn could modify the magnetic wave vector from $(\pi/a,0)$ to $(\pi/a,\pi/a)$ (square lattice unit cell with Fe ions at the vertices) [16], leading to a weakening of $s_\pm$-wave pairing [17]. However, the absence of single crystals with a size appropriate for neutron scattering experiments makes the determination of the magnetic correlations developing upon Mn doping rather difficult for Ln1111 superconductors.

Since in Fe-based superconductors one of the most likely pairing mechanisms involves magnetic excitations [18], it is of major importance to investigate how the spin excitations evolve in optimally doped $LaFe_{1-x}Mn_xAsO_{0.89}F_{0.11}$ superconductors as the QCP is approached. From ^{75}As nuclear spin-lattice relaxation rate $1/T_1$ measurements it was observed [14] that when T_c vanishes for $x_c \simeq 0.002$ the spin correlations follow the behavior predicted for strongly correlated electron systems close to a two-dimensional (2D) antiferromagnetic QCP [19]. In this Rapid Communication it is shown that upon increasing the chemical pressure, by partially substituting Y for La, T_c decreases more slowly with x (Fig. 1), mimicking the effect observed for Sm1111. This indicates that the different behavior of Sm1111 and La1111 against Mn impurities has to be associated with the larger chemical pressure induced by the lanthanide ions on the FeAs planes in the former case. From ^{19}F NMR $1/T_1$ measurements it is shown that besides the high frequency (10^{12}–10^{13} s^{-1}) dynamics probed by ^{75}As nuclei, an additional very low-frequency (megahertz range)

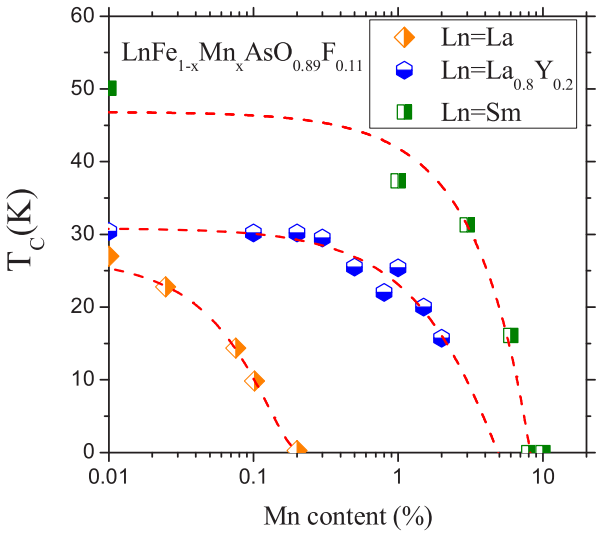

FIG. 1. (Color online) Superconducting phase diagram for $LaFe_{1-x}Mn_xAsO_{0.89}F_{0.11}$ [14], $La_{0.8}Y_{0.2}Fe_{1-x}Mn_xAsO_{0.89}F_{0.11}$, and $SmFe_{1-x}Mn_xAsO_{0.89}F_{0.11}$ [7,8] vs Mn content. Dashed lines are guides to the eye.

dynamics develops upon Mn doping and becomes progressively enhanced as the QCP is approached. Furthermore, it is evidenced that if the system is driven away from the QCP by partially substituting La with Y the low-frequency dynamics becomes significantly enhanced only at high Mn contents where $T_c \to 0$. These results evidence that the disruption of the superconducting phase coincides with the enhancement of low-frequency fluctuations possibly competing with the ones driving the pairing.

NMR experiments were performed on (La,Y) $Fe_{1-x}Mn_xAsO_{0.89}F_{0.11}$ polycrystalline samples. Y for La substitution allows one to vary the chemical pressure without introducing paramagnetic lanthanide ions which would significantly affect ^{19}F NMR $1/T_1$ [20]. Two series of samples were studied: the first one with no Y and with Mn contents of $x = 0\%$, 0.025%, 0.075%, 0.1%, and 0.2% (referred to as LaY0), while the second one was studied with 20% of yttrium (LaY20 hereafter) and Mn content $x = 0\%$, 0.3%, 0.5%, 10%, and 20%. LaY0 and LaY20 samples were prepared as described in Refs. [13] and [21], respectively. All the samples were optimally electron doped with fluorine content around 11% [22]. T_c was determined by means of superconducting quantum interference device (SQUID) zero-field-cooled magnetization measurements in a 10 Oe magnetic field [21]. The diagram of the superconducting phase, for both series of samples, as a function of Mn content is shown in Fig. 1. It is evident that the introduction of 20% of yttrium stabilizes the superconducting phase, leading to an increase of T_c for $x = 0$ [23] as well as to a marked increase of x_c from 0.2% to about 4.5%.

^{19}F NMR measurements were performed at low magnetic fields, $H \leqslant 1.5$ T, by using standard radio-frequency pulse sequences. The spin-lattice relaxation rate was estimated by following the recovery of nuclear magnetization $M_z(\tau)$ after a saturation recovery sequence. The recovery was fit

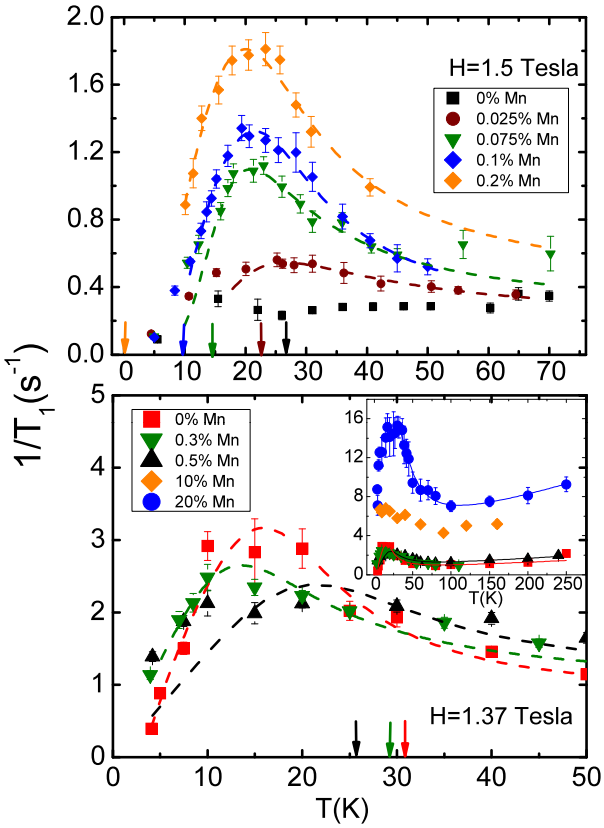

FIG. 2. (Color online) Top: Temperature dependence of ^{19}F NMR $1/T_1$ for LaY0 with x up to 0.2%. Bottom: Temperature dependence of ^{19}F NMR $1/T_1$ in LaY20 for Mn contents up to $x = 0.5\%$. In the inset the temperature (T) dependence is reported also for $x = 10\%$ and $x = 20\%$ nonsuperconducting samples. The dashed lines are fits of the data according to Eq. (3) in the text, while the arrows indicate the T_c of the different samples (decreasing with increasing x).

according to

$$M_z(\tau) = M_0[1 - f\, e^{-(\tau/T_1)^{\beta}}] \qquad (1)$$

with M_0 the magnetization at equilibrium. The factor $f \simeq 1$ is introduced to account for incomplete saturation and β is a stretching exponent which indicates a distribution of $1/T_1$. The stretching exponent β was found to be 1 for $T > 80$ K and decreased to about 0.5 at low T. The distribution of relaxation rates originates from the presence of different inequivalent Mn impurity configurations around ^{19}F nuclei.

The T dependence of $1/T_1$ for both sample series is shown in Fig. 2. Below 70 K ^{19}F NMR $1/T_1$ is characterized by a progressive increase upon decreasing T, by a pronounced maximum around 20 K, which can be either below or above T_c depending on the Y and Mn content (see Fig. 1) and eventually by a decrease at low T. Since, in all samples, the increase starts well above T_c those peaks should not be associated with dynamics which develop in the superconducting phase (e.g., vortex motions) [24] but to normal state low-energy excitations. It should be remarked that in the normal phase of Ln1111 superconductors without impurities no marked peak in $1/T_1$ has ever been reported. Only peaks in $1/T_1T$ have been observed [25], corresponding to small bumps in $1/T_1$. Here it

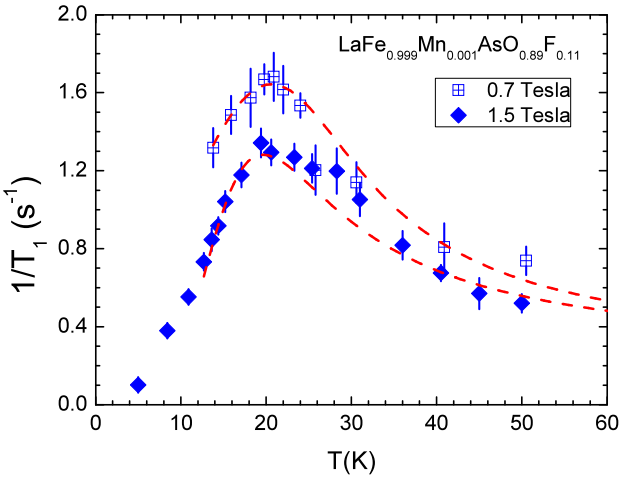

FIG. 3. (Color online) ^{19}F NMR $1/T_1$ in the $x = 0.1\%$ LaY0 sample at two different magnetic fields: 0.7 and 1.5 T. Dashed lines are fits according to Eq. (3).

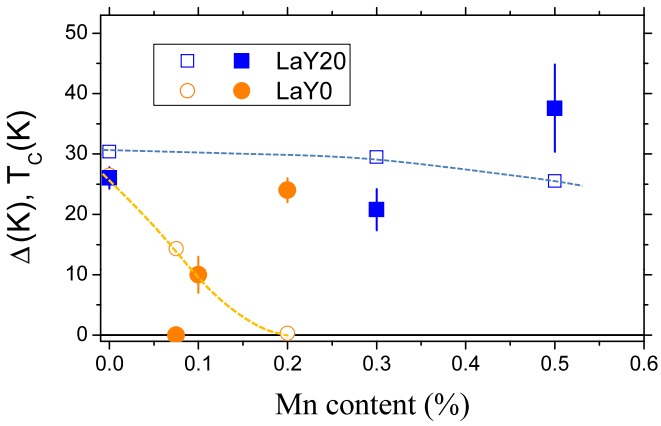

FIG. 4. (Color online) The width of the distribution of energy barriers Δ (closed symbols) and T_c (open symbols) are reported for the LaY0 and LaY20 samples. $\tau_0 = 3 \pm 2 \times 10^{-10}$ s for both families, while $\langle E_a \rangle = 47$ K fixed for LaY0 and $\langle E_a \rangle = 33 \pm 8$ K for LaY20 compounds.

is noticed that those peaks are significantly enhanced by the presence of impurities suggesting that Mn tends to strengthen those low-frequency dynamics which might already be present in pure compounds (see Fig. 2).

By performing $1/T_1$ measurements at different magnetic fields one observes that while the high T behavior is only weakly field dependent the magnitude of the peak around 20 K grows by lowering the magnetic field (Fig. 3). This is exactly the behavior expected in the presence of dynamics approaching the nuclear Larmor frequency ω_0, namely, in the megahertz range. If one assumes an exponential decay for the correlation function describing the fluctuations with a characteristic time τ_c, then one has [26]

$$\frac{1}{T_1} = \gamma^2 \langle h_\perp^2 \rangle \frac{\tau_c}{1 + \omega_0^2 \tau_c^2}, \tag{2}$$

where γ is the nuclear gyromagnetic ratio and $\langle h_\perp^2 \rangle$ the mean square amplitude of the local field fluctuations perpendicular to H. In several disordered systems, including cuprates [27], the T dependence of the correlation time is well accounted for by an Arrhenius law $\tau_c(T) = \tau_0 \exp(E_a/k_B T)$ with E_a an energy barrier and τ_0 the characteristic attempt time. Nevertheless, a monodispersive behavior cannot suitably describe the broad peaks in $1/T_1$ and one rather has to consider a distribution of correlation times associated with the nonuniform distribution of Mn impurities. This corresponds to a distribution of energy barriers which, for simplicity, was taken as squared with a width Δ centered around $\langle E_a \rangle$ [28]. In order to account for the high T behavior of $1/T_1$ a linear Korringa term αT [29], characteristic of metallic systems, was introduced (see Fig. 2). Then $1/T_1$ can be described by the expression [28]

$$\frac{1}{T_1} = \frac{\gamma^2 \langle h_\perp^2 \rangle T}{2\omega_0 \Delta} \left[a \tan\left(\omega_0 \tau_0 e^{(\langle E_a \rangle + \Delta)/T}\right) - a \tan\left(\omega_0 \tau_0 e^{(\langle E_a \rangle - \Delta)/T}\right) \right] + \alpha T. \tag{3}$$

By fitting the data of the superconducting samples ($x < 0.2\%$ for LaY0 and $x \leqslant 0.5\%$ for LaY20) one notices that for LaY0 spin correlations yield a significant increase in the width of the distribution on approaching the crossover between the superconducting and magnetic phases (Fig. 4). On the other hand, for the LaY20, within the uncertainty of the fit parameters, there is no evidence for a neat increase of Δ in the same doping range (Fig. 4). In other terms, in the LaY20 family the dynamics does not vary significantly upon increasing the Mn content up to $x = 0.5\%$, suggesting that the collective coupling is still weak.

Moreover, one may notice (Fig. 2) that for $x \leqslant 0.5\%$, in the LaY0 series the peak in $1/T_1$ grows significantly with Mn doping, while in the LaY20 series it remains practically unchanged. This evidences that $1/T_1$ increases progressively as $T_c \to 0$, namely, the strength of the local spin susceptibility in the FeAs plane becomes enhanced due to the proximity to the QCP. In other terms, for similar Mn contents the spin correlations get weaker as the chemical pressure is increased by Y doping. Further support in this respect is provided by the T dependence of ^{19}F NMR linewidth $\Delta\nu$ which is directly related to the amplitude of the staggered magnetization developing around the impurity [12]. As shown in Fig. 5 for similar Mn doping ^{19}F NMR linewidth is unambiguously larger in the sample without Y. The data in Fig. 5 can be fitted with a Curie-Weiss law $\Delta\nu = (\Delta\nu)_0 + C/(T + \Theta)$. $(\Delta\nu)_0 \simeq 13$ kHz is the T-independent linewidth due to nuclear dipole-dipole interaction which is assumed similar for both samples, since it is determined by nuclear dipolar coupling which remains practically unchanged (the F content and the lattice parameters do not vary significantly between the two samples [30]). This value is quite close to 14 kHz, the one estimated from dipolar lattice sums [31]. The fit of the data shows that C increases by a factor of 3 and that Θ increases from about 3 K to 11 K between the $x = 0.3\%$ LaY20 and $x = 0.2\%$ LaY0 samples.

The observation that the magnetic correlations become depressed when La is substituted by a smaller lanthanide ion can in principle be associated with a decrease of the ratio U/t between Coulomb repulsion and hopping integral due to the increase in the chemical pressure. However, for stripe collinear order [$\vec{Q} = (\pi/a, 0)$ or $(0, \pi/a)$] theoretical works [32,33]

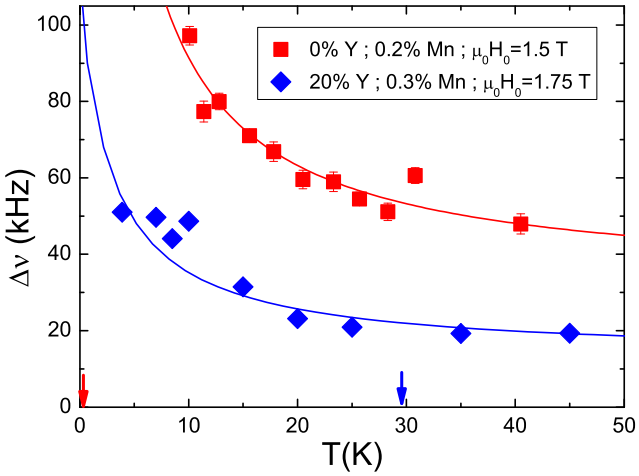

FIG. 5. (Color online) ^{19}F NMR line full width at half maximum $\Delta\nu$ in the $x = 0.2\%$ LaY20 sample (blue diamonds) and in the LaY0 $x = 0.3\%$ sample (red squares). Solid lines are best fits according to a Curie-Weiss law (see text), while the arrows indicate the T_c of the two samples.

suggest that in Ln1111 the magnetic order parameter should become enhanced on decreasing the Ln size or equivalently increasing the As z/c coordinate, exactly the opposite of what is found here. It should also be remarked that the behavior found upon Mn doping is contrary to that observed in Ru-substituted Fe-based superconductors where the magnetic order is stabilized by decreasing the size of the lanthanide [11]. Hence, it is likely that upon increasing x magnetic correlations different from the stripe ones develop. Giovannetti *et al.* [33] showed, through Landau free energy calculations, that around optimal electron doping the energy difference between the stripe and orthomagnetic phases becomes reduced. Hence, it might be possible that the introduction of Mn impurities could stabilize the latter type of order.

More recently Gastiasoro and Andersen [34] have considered the cooperative behavior of paramagnetic impurities coupled via Ruderman-Kittel-Kasuya-Yosida interaction in the Fe-based superconductors. They pointed out that upon increasing the Kondo-like coupling between the localized impurity and the itinerant electrons, Néel [$\vec{Q} = (\pi/a,\pi/a)$] correlations would arise and the amplitude of collinear stripe modes decrease. However, even when the coupling becomes significant and Néel fluctuations enhanced, stripe spin correlations would still survive. In a real space description their results imply the development of Néel-type correlations in small islands around the impurity and stripe spin arrangement at larger distances from the impurity. Even if from ^{19}F NMR spectra we cannot check the validity of this model, this theoretical approach is able to explain both the weakening of the superconductivity [17] and the onset of a novel magnetic phase upon Mn doping [14]. In such a scenario the peaks in $1/T_1$ should be associated with the freezing of the spin fluctuations around Mn impurities which get more and more correlated as the QCP is approached. The theoretical model by Gastiasoro and Andersen [34] also allows one to make an analogy between heavy fermion physics and that achieved by doping Fe-based superconductor impurities. In this respect we recall that, similarly to heavy fermions, at the QCP there is a charge localization [13] suggesting a divergence of the electron effective mass. Hence, one should actually consider two possible concomitant effects which depress superconductivity: loss of spin excitations causing the pairing and/or charge localization. Once more, we remark that the behavior achieved by Mn doping is quite different from that observed in Ln1111 superconductors doped with Ru spinless impurities, where even at very high doping levels ($\simeq$50%) the system remains metallic [35].

An alternative explanation for the growth of low-frequancy spin fluctuations in Mn-doped Ln1111 relies on the presence of nematic fluctuations. In this respect it is interesting to observe that even nominally pure samples do show a small bump in $1/T_1$ [25,36,37] in the same T range where the peak in ^{19}F NMR $1/T_1$ arises. The same low-frequency dynamics was found to affect the NMR transverse relaxation rate in $Ba(Fe_{1-x}Rh_x)_2As_2$ and was tentatively associated with nematic fluctuations [37], possibly involving charge stripes [36]. Although there is no neat evidence for the type of dynamics here, one may be tempted to relate the energy barrier probed by $1/T_1$ to the one separating the degenerate nematic phases [38]. In this framework the enhancement of the low-frequency dynamics could be associated with the pinning of those fluctuations by impurities.

In conclusion, the increase in the chemical pressure driven by Y for La substitution in $La_{1-y}Y_yFe_{1-x}Mn_xAsO_{0.89}F_{0.11}$ is found to lead to a less effective suppression of the superconducting ground state by Mn doping. ^{19}F NMR $1/T_1$ measurements exhibit a low-T peak which indicates the onset of very low-frequency dynamics with an amplitude directly related to the proximity of the compound to the QCP between superconducting and magnetic phases. Based on recent theoretical works, this behavior could be ascribed to the enhancement of spin correlations different from stripe ones, suggesting that T_c is depressed by the decrease in the spin fluctuations around $(\pi/a,0)$, which are widely believed to mediate the pairing, or by the localization effect in the region close to the metal-insulator boundary.

We would like to acknowledge useful discussions with Brian Andersen, Maria N. Gastiasoro, and J. Lorenzana and technical support by R. Wachtel, S. Müller-Litvani, and G. Kreutzer. This work was supported by MIUR-PRIN2012 Project No. 2012X3YFZ2, by the DFG through the SPP1458 in Project No. BU887/15-1 and SFB1143, and by the Emmy-Noether program (Grant No. WU595/3-1).

[1] H. Alloul, J. Bobroff, M. Gabay, and P. J. Hirschfeld, Rev. Mod. Phys. **81**, 45 (2009).

[2] J. S. Parker, D. E. Read, A. Kumar, and P. Xiong, Europhys. Lett. **75**, 950 (2006).

[3] M. A. McGuire, D. J. Singh, A. S. Sefat, B. C. Sales, and D. Mandrus, J. Solid State Chem. **182**, 2326 (2009).
[4] Y. Yiu, V. O. Garlea, M. A. McGuire, A. Huq, D. Mandrus, and S. E. Nagler, Phys. Rev. B **86**, 054111 (2012).
[5] Y. Yiu, P. Bonfá, S. Sanna, R. De Renzi, P. Carretta, M. A. McGuire, A. Huq, and S. E. Nagler, Phys. Rev. B **90**, 064515 (2014).
[6] P. Bonfá, P. Carretta, S. Sanna, G. Lamura, G. Prando, A. Martinelli, A. Palenzona, M. Tropeano, M. Putti, and R. De Renzi, Phys. Rev. B **85**, 054518 (2012).
[7] M. Sato and Y. Kobayashi, Solid State Commun. **152**, 688 (2012).
[8] E. Satomi, S. C. Lee, Y. Kobayashi, and M. Sato, J. Phys. Soc. Jpn. **79**, 094702 (2010).
[9] S. C. Lee, E. Satomi, Y. Kobayashi, and M. Sato, J. Phys. Soc. Jpn. **79**, 023702 (2010).
[10] S. Sanna, P. Carretta, P. Bonfá, G. Prando, G. Allodi, R. De Renzi, T. Shiroka, G. Lamura, A. Martinelli, and M. Putti, Phys. Rev. Lett. **107**, 227003 (2011).
[11] S. Sanna, P. Carretta, R. De Renzi, G. Prando, P. Bonfà, M. Mazzani, G. Lamura, T. Shiroka, Y. Kobayashi, and M. Sato, Phys. Rev. B **87**, 134518 (2013).
[12] D. LeBoeuf, Y. Texier, M. Boselli, A. Forget, D. Colson, and J. Bobroff, Phys. Rev. B **89**, 035114 (2014); Y. Texier, Y. Laplace, P. Mendels, J. T. Park, G. Friemel, D. L. Sun, D. S. Inosov, C. T. Lin, and J. Bobroff, Europhys. Lett. **99**, 17002 (2012).
[13] M. Sato, Y. Kobayashi, S. C. Lee, H. Takahashi, E. Satomi, and Y. Miura, J. Phys. Soc. Jpn. **79**, 014710 (2010).
[14] F. Hammerath, P. Bonfá, S. Sanna, G. Prando, R. De Renzi, Y. Kobayashi, M. Sato, and P. Carretta, Phys. Rev. B **89**, 134503 (2014).
[15] M. N. Gastiasoro and B. M. Andersen, arXiv:1502.05859.
[16] G. S. Tucker, D. K. Pratt, M. G. Kim, S. Ran, A. Thaler, G. E. Granroth, K. Marty, W. Tian, J. L. Zarestky, M. D. Lumsden, S. L. Bud'ko, P. C. Canfield, A. Kreyssig, A. I. Goldman, and R. J. McQueeney, Phys. Rev. B **86**, 020503 (2012).
[17] R. M. Fernandes and A. J. Millis, Phys. Rev. Lett. **110**, 117004 (2013).
[18] I. I. Mazin, D. J. Singh, M. D. Johannes, and M. H. Du, Phys. Rev. Lett. **101**, 057003 (2008); K. Kuroki, S. Onari, R. Arita, H. Usui, Y. Tanaka, H. Kontani, and H. Aoki, *ibid.* **101**, 087004 (2008); J. Zhang, R. Sknepnek, R. M. Fernandes, and J. Schmalian, Phys. Rev. B **79**, 220502 (2009).
[19] A. Ishigaki and T. Moriya, J. Phys. Soc. Jpn. **65**, 3402 (1996).
[20] G. Prando, P. Carretta, A. Rigamonti, S. Sanna, A. Palenzona, M. Putti, and M. Tropeano, Phys. Rev. B **81**, 100508 (2010).
[21] See Supplemental Material at http://link.aps.org/supplemental/10.1103/PhysRevB.92.020505 for the synthesis and characterization of LaY20 samples and for ^{19}F NMR spectra.
[22] For the LaY0 samples no variation of the intensity of the ^{19}F-NMR resonance line was found within the error bars, confirming that the intrinsic F content does not differ among the samples within ± 0.005.
[23] M. Tropeano, C. Fanciulli, F. Canepa, M. R. Cimberle, C. Ferdeghini, G. Lamura, A. Martinelli, M. Putti, M. Vignolo, and A. Palenzona, Phys. Rev. B **79**, 174523 (2009).
[24] L. Bossoni, P. Carretta, A. Thaler, and P. C. Canfield, Phys. Rev. B **85**, 104525 (2012); A. Rigamonti, F. Borsa, and P. Carretta, Rep. Prog. Phys. **61**, 1367 (1998).
[25] F. Hammerath, U. Gräfe, T. Kühne, H. Kühne, P. L. Kuhns, A. P. Reyes, G. Lang, S. Wurmehl, B. Büchner, P. Carretta, and H.-J. Grafe, Phys. Rev. B **88**, 104503 (2013).
[26] N. Bloembergen, E. M. Purcell, and R. V. Pound, Phys. Rev. **73**, 679 (1948).
[27] M.-H. Julien, F. Borsa, P. Carretta, M. Horvatić, C. Berthier, and C. T. Lin, Phys. Rev. Lett. **83**, 604 (1999).
[28] M. Filibian and P. Carretta, T. Miyake, Y. Taguchi, and Y. Iwasa, Phys. Rev. B **75**, 085107 (2007).
[29] C. P. Slichter, *Principles of Magnetic Resonance*, 3rd ed. (Springer, Berlin, 1990).
[30] Lattice parameters change by less than 0.5% between the LaY0 and the LaY20 series (see also the Supplemental Material), yielding a change by less than 1.5% in the contribution of dipolar interaction to the linewidth.
[31] About 84% of the second moment is due to F-La nuclear dipole interaction and about 13% to F-F interaction, while a minor contribution arises from F-As interactions.
[32] S. Sharma, S. Shallcross, J. K. Dewhurst, A. Sanna, C. Bersier, S. Massidda, and E. K. U. Gross, Phys. Rev. B **80**, 184502 (2009).
[33] G. Giovannetti, C. Ortix, M. Marsman, M. Capone, J. van den Brink, and J. Lorenzana, Nat. Commun. **2**, 398 (2011).
[34] M. N. Gastiasoro and B. M. Andersen, Phys. Rev. Lett. **113**, 067002 (2014).
[35] M. Tropeano, M. R. Cimberle, C. Ferdeghini, G. Lamura, A. Martinelli, A. Palenzona, I. Pallecchi, A. Sala, I. Sheikin, F. Bernardini, M. Monni, S. Massidda, and M. Putti, Phys. Rev. B **81**, 184504 (2010).
[36] L. Bossoni, P. Carretta, W. P. Halperin, S. Oh, A. Reyes, P. Kuhns, and P. C. Canfield, Phys. Rev. B **88**, 100503 (2013).
[37] A. P. Dioguardi, M. M. Lawson, B. T. Bush, J. Crocker, K. R. Shirer, D. M. Nisson, T. Kissikov, S. Ran, S. L. Bud'ko, P. C. Canfield, S. Yuan, P. L. Kuhns, A. P. Reyes, H.-J. Grafe, and N. J. Curro, arXiv:1503.01844.
[38] R. M. Fernandes and J. Schmalian, Supercond. Sci. Technol. **25**, 084005 (2012).